Evaluation of a new gamma emission imaging system and method for nuclear waste in nuclear power plant environments

J. Joung [a)1], N. Hung [a)], Y. K. Kim [a)], K. H. Bae [a)], J.M. Park [b)2], K.Y. Kim [b)], and J.W. Lim [b)]

Abstract– We have developed a new radiation imaging method and system and it provides visualization of 2D or pseudo 3D distributions of gamma emitting sources selected along with superimposed CCD images.

The main principle of the imaging method is recovering resolution degradation caused by attenuation and using an ultra-high sensitive collimation. This is achieved by applying deconvolution of the system response function.

To validate the performance of the new method within a real environment setup, we have conducted evaluation studies of various objects in controlled nuclear waste storage areas in nuclear power plants.

The imaging system successfully demonstrated visualizing of contaminated hot spot locations with corresponding isotopes ID and activity.

The new imaging technique and system are able to provide cost-effective solutions in the field of decommissioning, separation and decontamination of nuclear waste, and 24/7 radiation-leak monitoring of sites in NPP.

I. INTRODUCTION

Many efforts have been made since a couple of decades ago to utilize gamma emission imaging techniques used in nuclear medicine to image radiation distributions in radiological environment, for example, power plant monitoring, radiation waste management, cargo inspection, radiation contamination monitoring, environmental monitoring, and etc. [1-11].

Some of researches led to commercialization of "RadScan" series products by RMD instruments, LLC (MA, USA). Other commercially available products for imaging radiological environment include "GammaCam™" from US Department of Energy [3] and "RadScan® 800" by BIL Solutions Ltd. (UK).

Most recently, CZT detector based radiation imaging systems are commercialized. i.e., "iPIX" by Canberra (USA) and "Polaris" by H3D (USA).

However, the proposed prior methods and commercial products have not been widely accepted for imaging radiological environment because of critical limitations in sensitivity.

We have developed a new radiation imaging method and system for hot-spot imaging in radiological environments that overcomes limitations of conventional technologies [14-15]. It provides visualization of 2D or pseudo 3D distributions of gamma emitting sources selected along with superimposed CCD image(s).

To validate the performance of the method and system within a real environment setup, we have conducted an evaluation of radiation imaging of various targets in controlled nuclear waste storage areas of a nuclear power plant (Kori NPP, Pusan, Korea).

The imaging system successfully demonstrated finding contaminated hot spot locations with corresponding isotopes and activity within the nuclear wastes and pipes.

II. METHODS

2-1. Detector module and Imaging system

Majority of conventional gamma emission imaging techniques used in radiological environment are derivate from either gamma camera or Compton scatter imaging principle.

However, the difference in our approach over conventional methods is its simple detector configuration. The imaging detector module is consists of two simple components: a single-channel radiation detector (typically, 2x2 inch NaI(Tl)) with a flat field of view collimator which confines the FOV(field of view) to ±30° and a device that enables fan/tilt motion of the detector.

This simplified configuration provides not only ultra-high sensitivity but also cost-effectiveness.

Figure 1-(a) shows the imaging system with a CCD camera mounted on a fan/tilt device which enables raster scanning. 1-(b) shows a graphical representation of the detector module, i.e., 2x2 inch NaI is encapsulated within a cylindrical collimator which defines FOV at ±30°.

The wide open collimation enables ultra-high sensitivity but causes too poor spatial resolution to identify hot spots. This is why resolution recovery algorithm has to be developed.

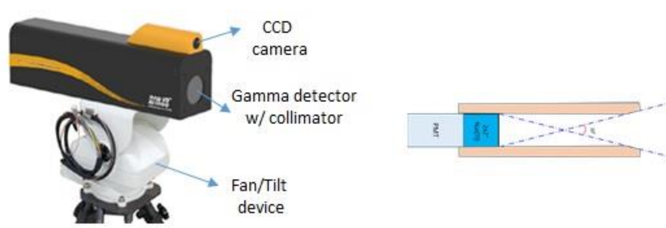

Figure 1. Detector module. (a) Imaging system mounted on tilt/fan device. (b) Graphical representation of detector module

[1] J. Joung, N. Hung, K. H. Bae and Y. K. Kim are with Nucare, Inc. Corresponding author: Jinhun Joung, Ph.D. (jinhun.joung@nucaremed.com).

[2] J. M. Park, K.Y. Kim and J. W. Lim are with KHNP, Inc. (Korea Hydro and Nuclear Power).

2-2. Imaging method

The brief imaging method is outlined as a flow chart in figure 2. Minimum of two projections measured at different angles are required to calculate the depth information of hot spots. Each projections are re-binned based on energy ROI and undergo several steps for resolution recovery followed by image reconstruction. MLEM based reconstruction is used in this studies.

The details are found in the reference [14].

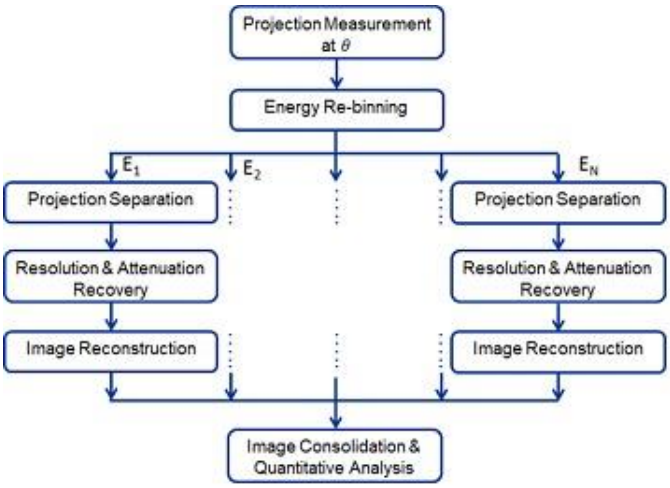

Figure2. Flow chart of proposed method.

The main principle of the imaging method is recovering resolution degradation caused by attenuation and using an ultrahigh-sensitive collimation. This is achieved by applying deconvolution of the system response function.

2-3. Experiment condition and setup

A total of 4 sites of nuclear waste storage were imaged and each site has different in background level (4 uSv/h ~ 23 uSv/h), object size/shape and contamination. In addition, the areas has uneven floors, different floor layouts, space limitation and obstacles. Therefore, the imaging configuration, i.e., system location and scan FOV was tailored for the conditions of each site.

Table 1 summarizes sampling condition of each measurement. Depend on object size and shape, the horizontal and vertical sampling range is determined. Then, sampling time at each view is determined based on the activity of object.

Fan/tilt device moving time of 30 sec from one position to next is not included in the total time.

Table 1. Measurement condition for each sites.

Sampling condition	Site #1	Site #2	Site #3	Site #4
Fan sample (degree)	(0°, 36°) (-30°, 0°)	(-12°, 30°) (-30°, 12°)	(-24°, 24°) (-24°, 24°)	(-27°, 27°) (-27°, 27°)
Up/down sample (degree)	(6°, -18°)	(-21°, 21°)	(18°, -18°)	(18°, -18°)
# Fsample	13	15	17	19
# UDsample	9	15	13	13
Time/sample (sec)	90	20	20	20
Total time (hour)	2.9	1.3	1.2	1.4

Figure 3 shows site photo and illustration of detectors setup of each sites. The imaging plan of each site is customized based on its target imaging volume, distance from detectors, orientation, floor layout and activity of objects.

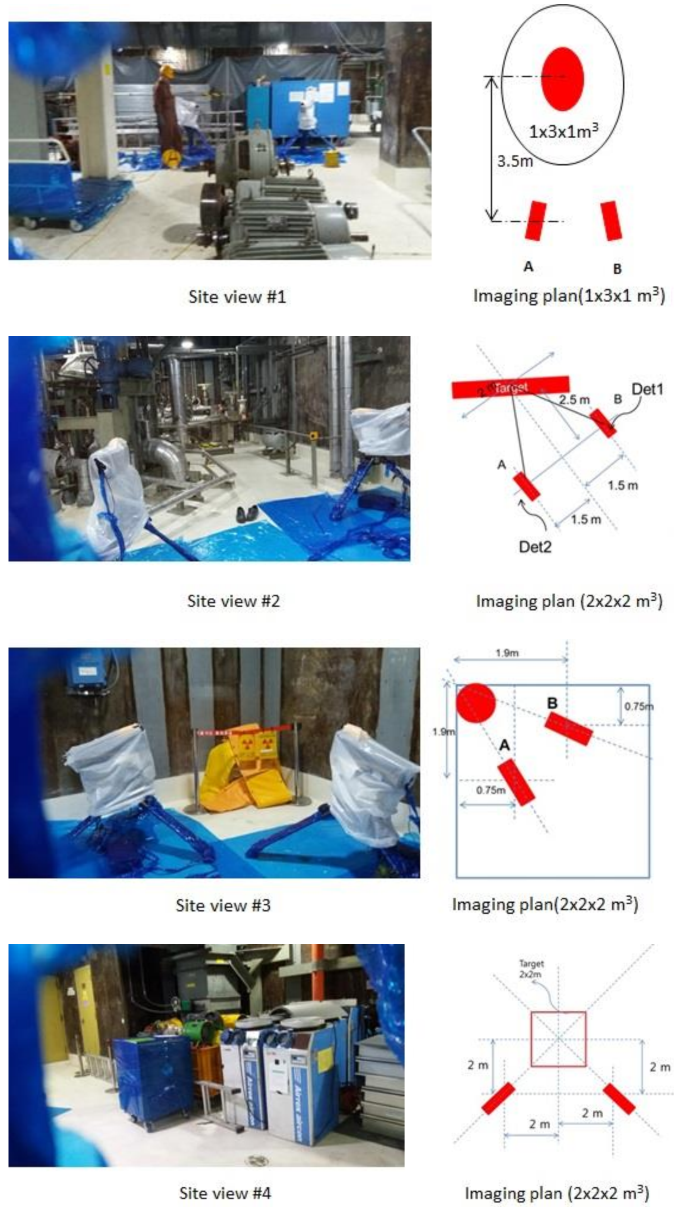

Fig.3. Site photos and customized imaging configuration for each sites.

III. Results

The new imaging system successfully demonstrates its imaging capability of nuclear wastes in NPP environment. Hot spot imaging performance of the 4 sites are summarized below.

3-1. Resolution recovery

Figure 4 shows original unprocessed images (top) and resolution revered images (bottom) of 4 sites. Each site has minimum of two projections from two detectors but only one selected image is shown in the figure for examples.

The location of contaminated hot spots are clearly identified and enhanced by the method. 4-(a) to (d) is corresponding to site #1 to #4, respectively.

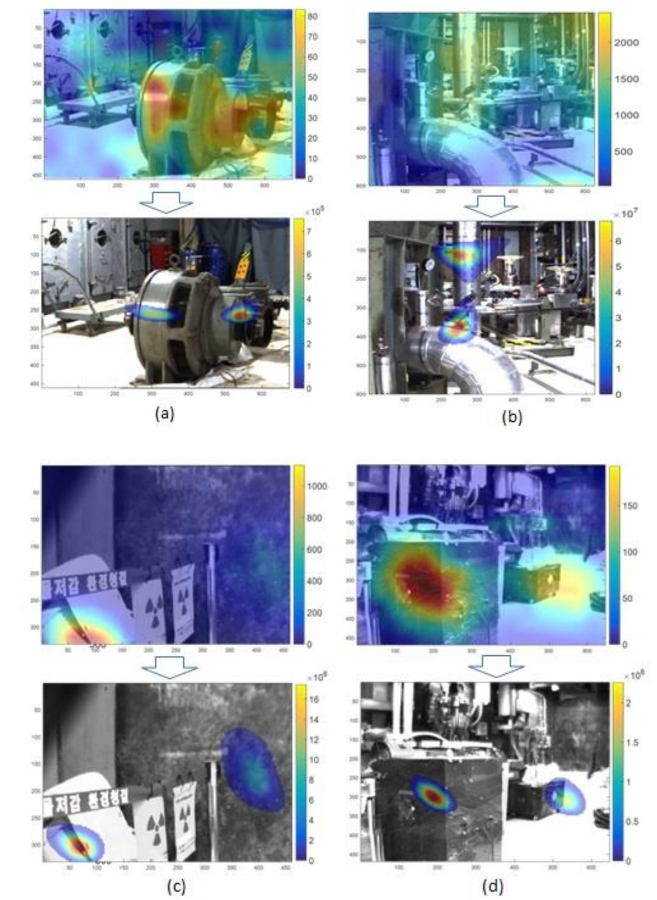

Figure 4. Resolution recovered images

Further quantitative analysis of the resolution recovery method are conducted. Profiles of hot-spot(s) from raw image and resolution recovered image are plotted in figure 5.

5-(a) and (b) represent measurement of site #4 by detector #1 and #2, respectively.

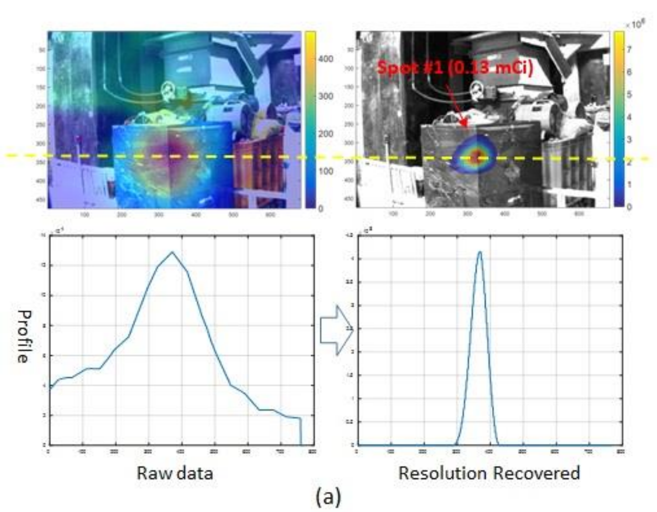

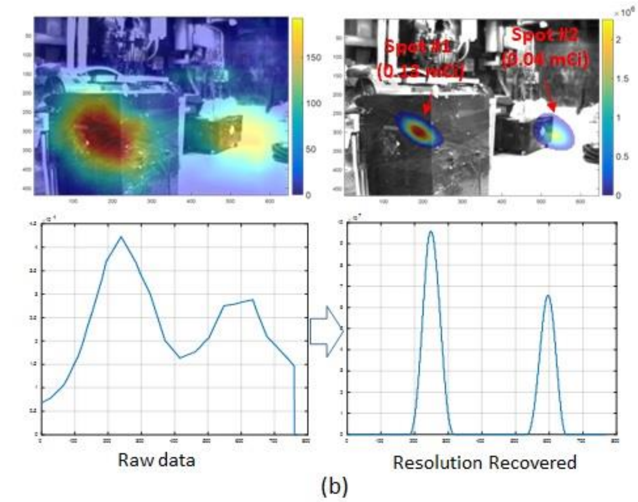

Figure 5. Profile analysis of hot spots

3-2. Spectroscopy and energy re-binned imaging

Spectroscopic feature of the system enables selective processing of data depending on the isotope of interest. This technique is refer to as “image re-binning”.

Figure 6 (a) and (b) shows two example wastes that are contaminated by a single isotope (Co-60) and multi isotopes (Co-60 and 775keV unknown), respectively.

Figure 6-(b) shows example of “re-binned” images based on its energy. Top images are 775 keV image and bottom one are Co-60 image.

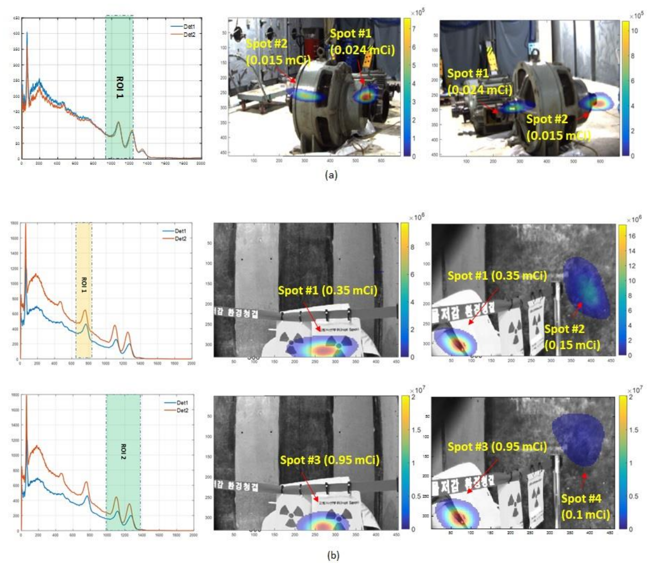

Fig.6. Spectrum and ROI example

3-3. Imaging performance summary

Figure 7 shows spectrums measured from all 4 sites. Each graph contains two spectrums from detector 1 and 2. All wastes are contaminated Co-60 and 7-(b), (c) and (d) have additional contamination from 775 keV gamma source.

The activity difference of the two detectors are due to the asymmetric location of the detector from the target and hot spots.

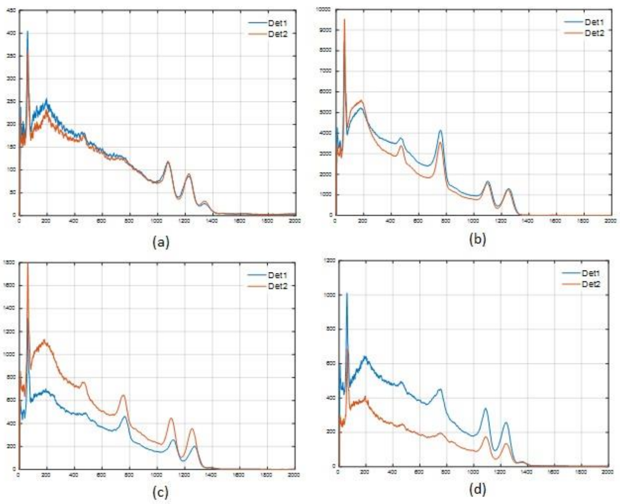

Figure 7. Spectrums measured from wastes in 4 sites.

Figure 8 is a site #1 where contaminated motors are stored. The sampling condition and imaging time were 13(H) x 9(V) scans with 3° interval at 90 seconds/view. Hot spots are clearly visualized by background compression and a hot spot enhancement technique.

Relatively small activity was found and the isotope was identified as Co-60 and the total activity was estimated as 24 uCi and 15 uCi for spots 1 and 2, respectively.

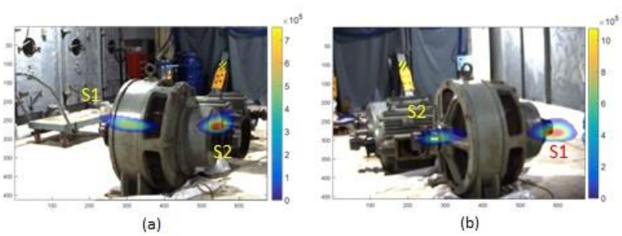

Fig.8. Site image of contaminated motors

Figure 9 is the case of a room filled with various size and shape of pipe lines. The sampling condition and imaging time were 15(H) x 15(V) scan with 3° interval at 20 seconds/view.

9-(a) is 775 keV image and activity were estimated as 1.2 mCi, 0.99 mCi and 0.41 mCi for spot1, 2 and 3, respectively. 9-(b) is Co-60 image with 1.50 mCi and 1.83 mCi for spot 4 and 5, respectively.

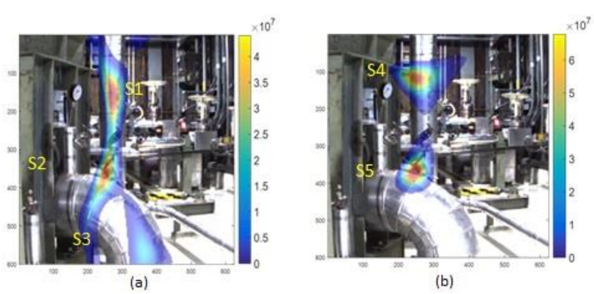

Fig.9. Site image of contaminated motors.

Figure 10 is the site of nuclear waste with high activity. The sampling condition and imaging time were 17(H) x 13(V) scans with 3° interval at 20 second/view.

10-(a) and (b) are 775 keV images and 10-(c) and (d) are processed Co-60 images.

The total activity of spots 1 and 2 in Figure 10-(a) and (b) were estimated as 0.36 mCi and 0.15 mCi, respectively.

The location of Co-60 hot spots are almost identical with 775 keV as shown in figure 10-(c) and (d). Activity were 0.95 mCi and 0.10 mCi for spots 3 and 4, respectively.

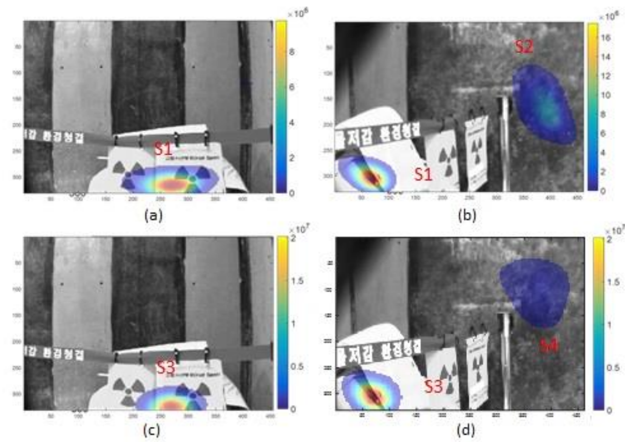

Fig.10. Site image of nuclear waste with high activity.

Figure 11 is the site image of contaminated equipment. The sampling condition and imaging time were 19(H) x 13(V) scans with 3° interval at 20 second/view.

11-(a) and (b) were identified as 775 keV and the total activity were estimated as 0.13 mCi and 0.04 mCi for spots 1 and 2, respectively.

11-(c) and (d) were Co-60 image with activity of 0.19 mCi and 0.03 mCi, respectively.

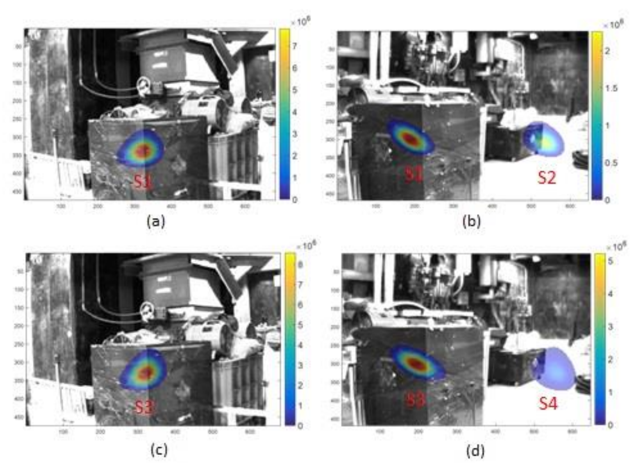

Fig.11. Site image of contaminated equipment.

IV. DISCUSSION

The weight of the detector module is about 38 kg including the fan/tilt device. And heavy collimator is the main contributor of its weight. Consequently, the high precision requirement of the fan/tilt device becomes critical factor so that it leads high price and heavier/bulkier device.

In addition, even though a high precision fan/tilt device is employed, detector dropping phenomena was unavoidable especially when the detector is tilted upward vertically. Long positioning time (about 30 sec) of the device from one view to another is another concerns.

Therefore, reducing the weight of the collimator is highly required. Researches are in progress to redesign the collimator such that reducing its length while maintaining desired FOV and sensitivity.

The proposed method requires at least two measurements from different view angles. However, if the depth (distance from detector to a hot spot) is known as prior information, single view is enough to generate a 2D projection with resolution recovered hot spots.

One can think of such application where radiation leak from a known location or device has to be continuously monitored. In such case, a single stationary system mounted on a wall or floor can conduct 24/7 monitoring by comparing the correlation between previous and current images.

V. CONCLUSION

Sensitivity is the most important factor in radiation imaging of radiological environment because, in general and relative to nuclear imaging, the imaging volume is big, distance from a detector to the activity source is long and detector efficiency is low.

We have developed a new imaging method and system that provides ultra-high sensitive while maintaining acceptable spatial resolution by recovery algorithm.

The method has been successfully demonstrated it capability of high sensitivity radiation imaging, spectroscopic analysis, and quantitative analysis of activity with real case studies in NPP environments.

The simplified configuration of the proposed detector module enables not only cost-effectiveness but also wide utilization in many applications including decommissioning planning of NPP, decontamination nuclear waste, leak monitoring in NPP field and more.

VI. REFERENCES

[1] "A combined video and gamma ray imaging system for robots in nuclear environments", R. Redus, M. Squillante, J Gorden, G Knoll and D. Wehe, Nuclear Instruments and Methods in Physics Research A 353 (1994) 324-327

[2] "A portable gamma camera for radiation monitoring", S. Guru, Z. Hee, D. Wehe and G. Knoll, IEEE Transactions on Nuclear Science, (1995) 367-370

[3] "GammaCam radiation imaging system". Deactivation and decommissioning focus area. Department of Energy. 1998.

[4] "Operation of the CARTOGAM portable gamma camera in a photon-counting mode", O. Gal, B. Dessus, F. Jean, F Laine and C. Leveque., IEEE Transactions on Nuclear Scinecne. Vol 48, No4, 2001.

[5] "A radiation monitoring system with capability of gamma imaging and estimation of exposure dose rate", W. Lee, G. Cho and H. Kim, IEEE Transactions on Nuclear Science, V49, N3 (2002) 1547-1551

[6] "Development of three-dimensional gamma camera with imaging plates and multi-pinhole collimators", N. Yamamura, A. Uritani, K. Watanabe, J. Kawarabayashi, T. Lguchi., Nuclear Instruments & Methods in Physics Research A. 505 (2003) 577-581

[7] "Development of coded-aperture imaging with a compact gamma camera", M. Gmar, O. Gal, C. Goaller, O. Ivanov, V. Potapov, V. Stepanov, F. Laine, F. Lamadie., IEEE NSS MIC 2004.

[8] "A gamma locator for remote radioactivity mapping and dose rate control", V. Potapov, N. Kononov, O. Ivanov, S. Ignatov, V. Stepanov, A. Chesnokov and V. Volkov., IEEE NSS MIC, 2004.

[9] "Advanced multi-dimensional imaging of gamma-ray radiation", M. Woodring, D. Beddingfield, D. Souza, G. Entine, M. Squillante, J. Christian and A. Kogan. Computer Physics Communications,

[10] "Portable Video/Gamma Camera for surveillance, safeguards, treaty verification and area monitoring, J. Christian, M Squillante, M. Woodring and G Entine., INMM meeting in Orlando Florida, 2004.

[11] "Design of wide energy range coded aperture mask of an environment radiation monitoring system", X. Li, Z. Wu, Y. Liu, T. Ma and Y. Jin., IEEE Nuclear Science Symposium Conference Record, 2007.

[12] "GAMPIX: a new gamma imaging system for radiological safety and homeland security purposes", F. Carrel and et. Al., IEEE NSS MIC 2011.

[13] "GAMPIX: a generation of gamma camera", M. Gmar, M. Agelou. F. Carrel and V. Schoepff., Nuclear Instruments and Methods in Physics Research A. 652 (2011), 638-640.

[14] "Radiation imaging method and system", J. Joung. US patent US 9,953,463 B2.

[15] "Investigation of innovative radiation imaging method and system for radiological environments", H. Nguyen, J. Joung, Y. Kim and K. Lee, Nuclear Instruments and Methods in Physics Research A 847 (2017) 15-28.